

# Timing diagrams and correlations in gamma-ray bursts signal jets from accretion into black holes

S. McBreen, B. McBreen, F. Quilligan, and L. Hanlon

Department of Experimental Physics, University College Dublin, Dublin 4, Ireland

Received 22 October 2001 / Accepted 10 December 2001

**Abstract.** The temporal properties of a sample of 498 bright gamma-ray bursts (GRBs) with durations between 0.05 s and 674 s were analysed. The large range in duration ( $T_{90}$ ) is accompanied by a similarly large range in the median values of the pulse timing properties including rise time, fall time, FWHM and separation between the pulses. Four timing diagrams relating these pulse properties to  $T_{90}$  are presented and show the power law relationships between the median values of the 4 pulse timing properties and  $T_{90}$ , but also that the power laws depend in a consistent manner on the number of pulses per GRB. The timing diagrams are caused by the correlated properties of the pulses in the burst and can be explained by a combination of factors including the Doppler boost factor  $\Gamma$ , a viewing effect caused by a jet and different progenitors. GRBs with similar values of  $T_{90}$  have a wide range in the number of pulses. GRBs with the large number of short and spectrally hard pulses may occur either from a homogeneous jet with a higher average value of  $\Gamma$  or close to the axis of an inhomogeneous jet with higher values of  $\Gamma$  near the rotation axis. The less luminous GRBs with fewer pulses may originate further from the axis of the inhomogeneous jet. The pulses in GRBs have six distinctive statistical properties including correlations between time intervals, correlations between pulse amplitudes, an anticorrelation between pulse amplitudes and time intervals, and a link to intermittency in GRS 1915+105. The timing diagrams and correlated pulses suggest that GRBs are powered by accretion processes signalling jets from the formation of black holes.

**Key words.** Gamma rays – bursts: Gamma rays – observations: Methods – data analysis: Methods – statistical

## 1. Introduction

The cosmological origin of gamma-ray bursts (GRBs) requires an extraordinary amount of energy to be emitted in gamma-rays (Piran, 1999). The source of this energy is thought to be a cataclysmic event involving mergers of compact objects such as neutron stars or a neutron star and black hole (Paczynski, 1991; Ruffert & Janka, 1999) or the formation of a black hole in massive stars (MacFadyen & Woosley, 1999; Popham et al., 1999). GRB light curves are complex and irregular (Fishman & Meegan, 1995) and a range of techniques have been developed to elucidate their structure (McBreen et al., 1994; Norris et al., 1996; Lee et al., 2000; Beloborodov et al., 2000; Quilligan et al., 2002). In this paper we present the results of the analysis of pulses in a large sample including long and short GRBs. The main results are presented in section 3 including four timing diagrams and our analysis of pulse properties. These results along with the unique properties of the pulses in GRBs are interpreted in section 4 and used to provide additional insights to the emission process and the central engine that support jets from accretion into newly formed black holes.

## 2. Pulse analysis in GRBs

The BATSE experiment has provided the most uniform collection of GRBs available. A large sample of the brightest GRBs with data combined from the four energy channels was analysed using either wavelets or median filters. A detailed account of this process has been described elsewhere (Quilligan et al., 2002; McBreen et al., 2001). An automated pulse selection algorithm was used to detect pulses in the denoised signals. The samples included the brightest 319 GRBs with  $T_{90} > 2$  s analysed at 64 ms resolution and 100 GRBs with  $T_{90} < 2$  s analysed at 5 ms resolution. To extend the sample to include GRBs with  $T_{90}$  well beyond 100 s, a further 79 bright GRBs were included and analysed at 256 ms resolution.

Pulses that were isolated from neighbouring pulses at  $\geq 50\%$  level were selected and the rise times  $t_r$ , fall times  $t_f$  and FWHM were measured. The time intervals between pulses  $\Delta T$ , above the  $5\sigma$  threshold, were determined. The individual distributions of  $t_r$ ,  $t_f$ , FWHM and  $\Delta T$  have a wide range and are consistent with lognormal distributions. The bursts were split into  $T_{90}$  categories with comparable number of pulses and typical lower boundaries 0, 0.5, 2, 15, 30 and greater than 100 s for the GRBs

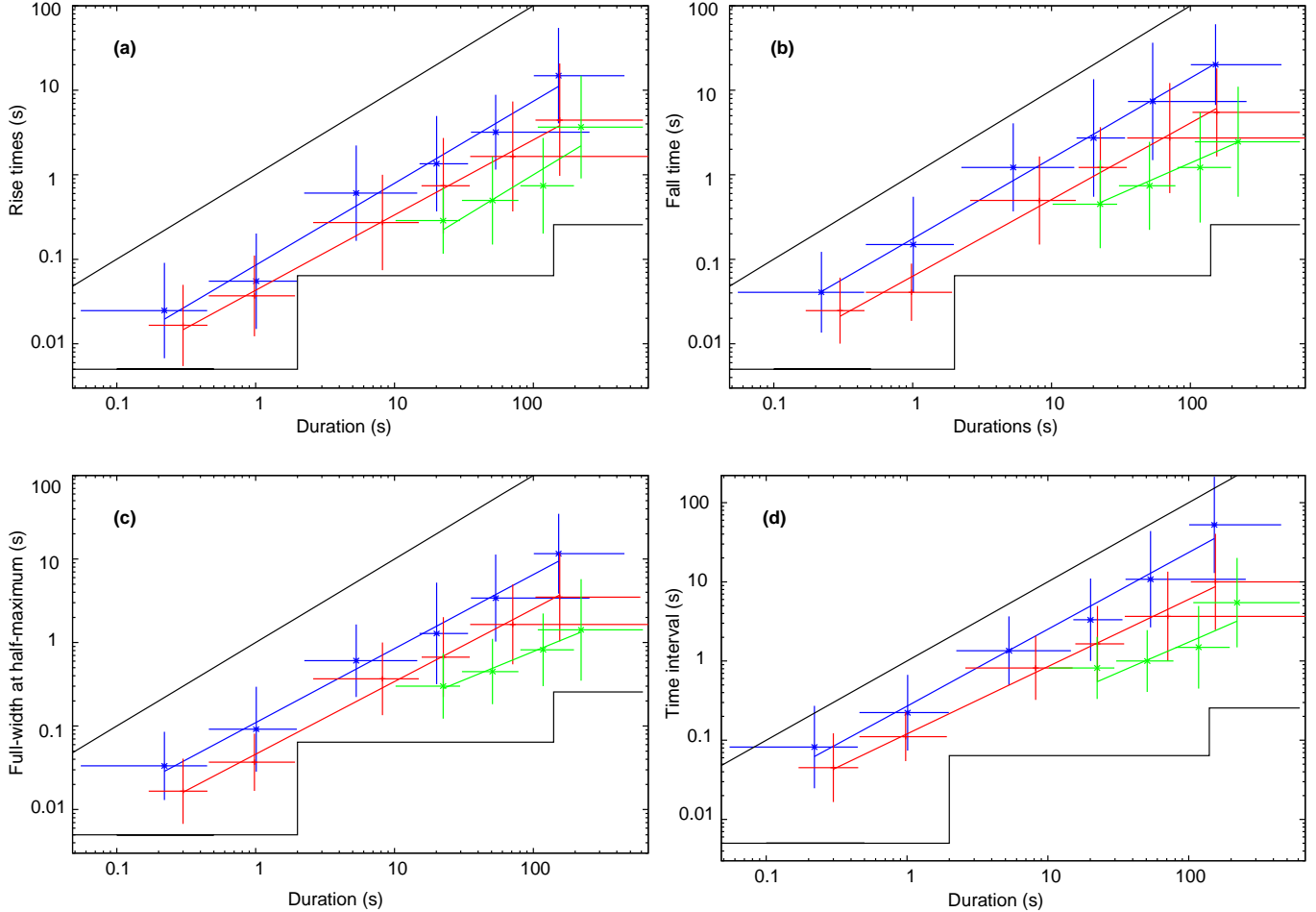


**Fig. 1.** The timing diagrams in GRBs. The median values obtained from the lognormal distributions for the pulse timing parameters (a)  $t_r$ , (b)  $t_f$ , (c) FWHM and (d)  $\Delta T$  are plotted versus duration  $T_{90}$  for GRBs in three categories i.e.  $1 \leq N \leq 3$  (blue),  $4 \leq N \leq 12$  (red) and  $N > 12$  (green). The crosses signify the range covered in  $T_{90}$  and  $e^{\mu \pm \sigma}$  for the lognormal distribution which includes 16% to 84% of the pulse values for that  $T_{90}$  bin. The upper diagonal line is the limit where the pulse parameter is equal to  $T_{90}$  and the lower lines by the limited time resolution i.e. 5 ms, 64 ms and 256 ms. In some GRBs with few pulses separated by a long  $\Delta T$  the value of  $T_{90}$  which goes from 5% to 95% of the counts may not include a small peak before or after the  $\Delta T$  yielding a value of  $\Delta T > T_{90}$ . This effect is seen in (d). Small corrections were applied to the pulse timing locations of the crosses that took into account the truncation of the distributions by the limited time resolution. The lines are the best fits to the median values and the power law indices are listed in Table 1. The timing values were obtained for pulses that were isolated from neighbouring pulses at  $\geq 50\%$  whereas all pulses above  $5\sigma$  were used for  $\Delta T$ .

at 256 ms resolution. The latter GRBs were binned separately despite the overlap with  $T_{90}$  because they are from a dimmer sample that was included to extend the range in duration to ultra-long GRBs. The GRBs were further split into three categories based on the number of pulses  $N \geq 5\sigma$  i.e.  $1 \leq N \leq 3$ ,  $4 \leq N \leq 12$  and  $N \geq 12$ . The median  $\mu$  and standard deviation  $\sigma$  of each lognormal distribution was determined (Quilligan et al., 2002).

### 3. Results

The diagrams of  $t_r$ ,  $t_f$ , FWHM and  $\Delta T$  versus  $T_{90}$  are presented in Fig. 1 for three categories based on the number of pulses in the GRBs. The crosses in Fig. 1 are not error bars but show the range in  $T_{90}$  over which the pulses in

the bursts were combined and the range of the lognormal distribution that includes 67% of the values for the relevant pulse property. The indices of the best fit power-laws to the median values in Fig. 1 are listed in Table 1 and all have values close to unity. The values of  $t_r$ ,  $t_f$ , FWHM and  $\Delta T$  are well correlated with each other (Quilligan et al.,

**Table 1.** Indices of the power law fits to the timing data.

Property	$1 \leq N \leq 3$	$4 \leq N \leq 12$	$N > 12$
Rise Time	$0.98 \pm 0.07$	$0.89 \pm 0.03$	$1.02 \pm 0.3$
Fall Time	$0.95 \pm 0.04$	$0.91 \pm 0.05$	$0.72 \pm 0.1$
FWHM	$0.89 \pm 0.04$	$0.87 \pm 0.03$	$0.68 \pm 0.06$
Time Interval	$0.97 \pm 0.06$	$0.85 \pm 0.03$	$0.77 \pm 0.27$

2002) which explains the similarity of the diagrams when plotted versus  $T_{90}$ . All four figures are presented to emphasise this result. For the two categories with  $1 \leq N \leq 3$  and  $4 \leq N \leq 12$  the power-laws between the median values of  $t_r$ ,  $t_f$ , FWHM,  $\Delta T$  and  $T_{90}$  extend over a range of more than  $10^3$  and includes GRBs from both sub-classes. The GRBs with  $N > 12$  include only those with  $T_{90} > 2$  s because  $N = 9$  is the largest value for GRBs with  $T_{90} < 2$  s. The data are displaced from the two categories of GRBs with fewer pulses and display flattening for  $T_{90} < 50$  s which may be caused by a selection effect because of pulse amalgamation by the 64 ms resolution of the data.

The properties of the isolated pulses in GRBs with  $T_{90} > 2$  s, at 64 ms resolution, were compared with the preceding ( $\Delta T^-$ ) and subsequent ( $\Delta T^+$ ) values of  $\Delta T$ . The pulse amplitudes (PA) are more anticorrelated with  $\Delta T^-$  than  $\Delta T^+$  with Spearman rank order correlation coefficients of -0.39 and -0.33. The peak to peak values of  $\Delta T$  were then corrected for the strong correlation between  $\Delta T$  and the pulse rise and fall times (Quilligan et al., 2002). The amended values of the correlation coefficients are -0.27 and -0.16 with probabilities that the anti-correlations arose by chance of  $10^{-15}$  and  $10^{-6}$ . This difference did not depend on the isolation level of the pulses which was varied from 30% to 80%. The FWHM of the pulses were also compared with  $\Delta T^-$  and  $\Delta T^+$  and found to be strongly correlated. The correlations were marginally stronger for  $\Delta T^-$  than  $\Delta T^+$ .

## 4. Discussion

The data in Fig. 1 shows that the median values of  $t_r$ ,  $t_f$ , FWHM and  $\Delta T$  depend strongly on  $T_{90}$  and also on the number of pulses. GRBs with the same durations can have a wide variation in the number of pulses and the pulse properties. GRBs with a small number of pulses generally have slow pulses that are further apart while bursts with larger number of pulses have faster and spectrally harder pulses that are closer together (Norris et al., 2001). In both cases the same pattern is observed except that the median values of  $t_r$ ,  $t_f$ , FWHM and  $\Delta T$  scale with  $T_{90}$ . Bursts with only one pulse and correlated pulse properties would lie on a line of slope unity, while bursts with many pulses lie on parallel lines if the pulse properties and  $\Delta T$  are correlated. The correlated nature of the pulse parameters and  $\Delta T$  provide additional information on the central engine and the emission process.

### 4.1. Number of pulses, pulse properties and jets

The separation of GRBs based on  $N$  (Fig. 1) suggests a kinematic origin because the median values of the pulse timing parameters and  $\Delta T$  scale in the same way and by about the same amount. In the internal shock model, an effect of this type may occur in homogeneous jet models where the degree of collimation and range in  $\Gamma$  depends on the mass at the explosion (Kobayashi et al., 2001) or in an inhomogeneous jet model by a viewing effect caused

by collimated emission with higher average values of  $\Gamma$  close to the rotation axis, where there is lower baryon pollution (Rees & Mészáros, 1994; Rees, 1999; Salmonson, 2000). The transparency radius of the fireball  $r_t$  varies as  $\Gamma^{-\frac{1}{2}}$ . The profiles of pulses in bursts from off-axis will be slowed by (1) the reduced value of  $\Gamma$  and (2) the longer time for faster shocks to catch slower ones before reaching  $r_t$ . There will be fewer shocks to collide outside  $r_t$  and hence generate lower luminosity bursts with slower and softer pulses because the additional shock amalgamation produces a narrower range in  $\Gamma$ . Indeed this process may be a key factor in controlling the spread in  $\Gamma$  in GRBs.

The luminosity of BATSE bursts is not determined but several factors imply that GRBs with faster and harder pulses are more luminous. The luminosity-variability and luminosity-lag correlations for GRBs with known  $z$  infer that the more variable and spectrally harder bursts are more luminous (Norris et al., 2000; Salmonson, 2000; Fenimore & Ramirez-Ruiz, 2001; Schaefer et al., 2001; Ioka & Nakamura, 2001; Schmidt, 2001). These correlations can be explained in an inhomogeneous jet model where the more luminous and variable bursts with higher  $N$  occur close to the axis and the slower, softer and less luminous bursts from further off-axis (Quilligan et al., 2002). In addition, there is the strong case for jets in GRBs based on the impressive range of afterglow studies (Frail et al., 2001). The unexpected effect is that the jet has left its imprint on the timing profile of the burst.

### 4.2. Variation of pulse properties and $\Delta T$ with $T_{90}$

The power laws in Fig. 1 connect the pulse data in the two sub-classes for  $1 \leq N \leq 3$  and  $3 \leq N \leq 12$ . The median values of the pulse timing parameters and  $\Delta T$  scale with  $T_{90}$  by about a factor of  $10^3$ . This result may indicate a direct connection between the two sub-classes of bursts or that they coincidentally lie on the same power laws in the absence of sufficient data to independently determine the slopes for the short bursts. The popular progenitors of GRBs range from mergers of compact objects such as neutron stars and black holes to collapsars and hypernovae in massive stars. A neat feature of most progenitor models is that they provide a generic scenario based on the formation of a black hole with a massive debris torus that is rapidly accreted and energises the jet by neutrino transport and magnetohydrodynamic processes.

The variation of the pulse parameters with  $T_{90}$  maybe caused by the same emission mechanisms and progenitors. If GRBs have the same progenitors, the short GRBs must have very high values of  $\Gamma$  to produce the short durations (Piran, 1999). The high value of  $\Gamma$  is close to the upper bound allowed by the internal shock model (Sari & Piran, 1997; Lazzati et al., 1999) but well below what can in principle be produced in a very low baryon environment (Mészáros & Rees, 1997). An alternative interpretation is that there are two types of progenitors with pulses that coincidentally lie on the same power laws. The progeni-

tors that arise from massive stars may not be capable of producing short GRBs. The short bursts may come from mergers of neutron stars or neutron stars and black holes (Ruffert & Janka, 1999) where the time structure in the bursts reflects the interaction of thin relativistic shocks with  $\Gamma \sim 100$  and duration of  $\sim 50$  ms. In this two progenitor scenario the high values of  $\Gamma$  can be reduced by about an order of magnitude. In addition the central engine and the environment before the photosphere may combine to smooth the shocks in a way that is a function of  $T_{90}$ .

#### 4.3. Correlations between pulses

There are a number of new results on pulses, from short and long GRBs, that constrain the emission process. These include (1) the distributions of values of  $t_r$ ,  $t_f$ , FWHM, pulse amplitude (PA) and pulse area of isolated pulses are not random but have lognormal distributions (Quilligan et al., 2002; McBreen et al., 2001; Nakar & Piran, 2001), (2) the values of  $\Delta T$  are lognormally distributed with a power-law excess of long time intervals or a Pareto-Levy tail for GRBs with  $T_{90} > 2$  s (Quilligan et al., 2002; McBreen et al., 2001; Nakar & Piran, 2001), (3) there is an anticorrelation between the values of PA and FWHM (Ramirez-Ruiz & Fenimore, 2000; Quilligan et al., 2002), (4) there is a positive correlation between the values of the PA that extend over many pulses (Quilligan et al., 2002; McBreen et al., 2001), (5) there is also a positive correlation between the values of  $\Delta T$  (Quilligan et al., 2002; McBreen et al., 2001), (6) the PA of isolated pulses in GRBs with  $T_{90} > 2$  s and 64 ms resolution were compared with  $\Delta T^-$  and  $\Delta T^+$  because of a strong correlation between the pulse width and  $\Delta T^-$  in the galactic superluminal source GRS 1915+105 where outbursts are powered by accretion into a black hole (Belloni et al., 1997) and a correlation between long quiescent periods in GRBs and subsequent intervals of emission (Ramirez-Ruiz & Merloni, 2001). The PAs were found to be anticorrelated with  $\Delta T^-$  and  $\Delta T^+$  with a slightly larger anticorrelation for  $\Delta T^-$ . Any additional correlations between the pulse properties and  $\Delta T^-$  would be expected to be much weaker than in GRS 1915+105 because a similar intermittent pattern in the outbursts from the central engine would have to persist after shock interactions generated the outbursts. The combination of the six results make the pulses in GRBs quite unique. In addition long pulses are asymmetric and reach their maximum earlier in higher energy bands while shorter pulses tend to be more symmetric with negligible time lags between energy channels (Norris et al., 1996).

The three results discussed above seem to favour an internal shock model powered by a hyper-accretion process into a newly formed black hole (Ruffert & Janka, 1999; Popham et al., 1999; Zhang & Fryer, 2001). The accretion process has been modelled and is sensitive to the rate at which material piles up around the black hole and the accretion time scale of the particles. The accretion rate might provide the overall control on the process

that eventually generates the correlated outbursts from the jet. The pulse amplitudes and time intervals can be coupled because higher accretion rates cause larger outbursts that are closer in time, while lower accretion rates produce smaller and slower events that are further apart. It appears that variation in the rate of accretion, the thickness of the relativistic shocks and the viewing angle of the jet may be key factors in accounting for the observed durations and pulse properties in GRBs. There are many uncertain factors that influence the process. These include the viscosity of the particles, the mass and angular momentum of the disk, the mass and spin of the black hole and the energy extraction and collimation process.

#### References

- Belloni, T., Mendez, M., King, A. R., van der Klis, M., & van Paradijs, J. 1997, *ApJ*, 488, L109  
 Beloborodov, A. M., Stern, B. E., & Svensson, R. 2000, *ApJ*, 535, 158  
 Fenimore, E. E. & Ramirez-Ruiz, E. 2001, *ApJ*, submitted, [astro-ph/0004176]  
 Fishman, G. J. & Meegan, C. A. 1995, *ARAA*, 33, 415  
 Frail, D. A., Kulkarni, S. R., Sari, R., et al. 2001, *ApJ*, 562, L55  
 Ioka, K. & Nakamura, T. 2001, *ApJ*, 554, L163  
 Kobayashi, S., Ryde, F., & MacFadyen, A. 2001, [astro-ph/0110080]  
 Lazzati, D., Ghisellini, G., & Celotti, A. 1999, *MNRAS*, 309, L13  
 Lee, A., Bloom, E., & Petrosian, V. 2000, *ApJS*, 131, 1  
 MacFadyen, A. I. & Woosley, S. E. 1999, *ApJ*, 524, 262  
 McBreen, B., Hurley, K. J., Long, R., & Metcalfe, L. 1994, *MNRAS*, 271, 662  
 McBreen, S., Quilligan, F., McBreen, B., Hanlon, L., & Watson, D. 2001, *A&A* 380, L31  
 Mészáros, P. & Rees, M. J. 1997, *ApJ*, 482, L29  
 Nakar, E. & Piran, T. 2001, [astro-ph/0103210]  
 Norris, J. P., Nemiroff, R. J., Bonnell, J. T. et al. 1996, *ApJ*, 459, 393  
 Norris, J. P., Marani, G. F., & Bonnell, J. T. 2000, *ApJ*, 534, 248  
 Norris, J. P., Scargle, J. D., & Bonnell, J. T. 2001, [astro-ph/0105052]  
 Paczynski, B. 1991, *Acta Astron.*, 41, 257  
 Piran, T. 1999, *Phys. Report*, 314, 575  
 Popham, R., Woosley, S. E., & Fryer, C. 1999, *ApJ*, 518, 356  
 Quilligan, F., McBreen, B., Hanlon, L., et al. 2002, *A&A*, 385, 377  
 Ramirez-Ruiz, E. & Fenimore, E. E. 2000, *ApJ*, 539, 712  
 Ramirez-Ruiz, E. & Merloni, A. 2001, *MNRAS*, 320, L25  
 Rees, M. J. 1999, *A&AS*, 138, L491  
 Rees, M. J. & Mészáros, P. 1994, *ApJ*, 430, L93  
 Ruffert, M. & Janka, H.-T. 1999, *A&A*, 344, 573  
 Salmonson, J. D. 2000, *ApJ*, 544, L115  
 Sari, R. & Piran, T. 1997, *MNRAS*, 287, 110

- Schaefer, B. E., Deng, M., & Band, D. L. 2001, ApJ, 563,  
L123
- Schmidt, M. 2001, ApJ, 552, 36
- Zhang, W. & Fryer, C. L. 2001, ApJ, 550, 357